

Cathodic Reactions Involved in the Corrosion of X80 steel in Acidic Soil Simulated Solution

Shuaixing Wang^{1,2,*}, Daoxin Liu¹, Nan Du², Qing Zhao², Jinhua Xiao²

¹ Institute of Corrosion and Protection, Northwestern Polytechnical University, Xi'an 710072, China

² School of Material Science and Technology, Nanchang Hangkong University, Nanchang 330063, China

*E-mail: wsxxpg@126.com

Received: 19 June 2016/ Accepted: 3 August 2016 / Published: 6 September 2016

Research on soil corrosion mainly focused on the impact of soil parameters on corrosion behavior, but the cathodic corrosion reaction of steel in acidic soil has not been studied systematically. In this work, the cathodic reaction involved in the corrosion of X80 steel in acidic soil simulated solution under various conditions were analyzed, along with data from hydrogen collection testing and the polarization curve. In the acidic soil simulated solution, the cathodic corrosion reaction of X80 steel depended on the combined effects of pH and dissolved oxygen (DO) concentration. For pH 5.0, oxygen-consuming corrosion occurred, and the corrosion rates in oxygen-adequate and anoxic system (0.90~0.25 ppm) depended on the oxygen ionization reaction and oxygen diffusion process, respectively. For pH 4.0 and DO >1.90 ppm, the depolarization of oxygen was still the main cathodic reaction, but hydrogen evolution dominated the cathodic process when DO was 0.25 ppm. In addition, both the reduction reactions of O₂ and H⁺ were present in the solution of pH 3.0, but the hydrogen reduction contribution was the key factor.

Keywords: X80 pipeline steel; Acidic soil; Corrosion; Cathodic reaction; Hydrogen evolution (HE)

1. INTRODUCTION

Corrosion of buried steel in soils is a vital threat to the safe operation of natural gas pipelines [1-5]. Although various parameters of steel corrosion in soils have been widely studied, including temperature, soil resistivity[6-7], soil moisture[8-9], soil salinity/pH/ porosity [10-11], redox potential and other physical factors [13-15], the research has so far mainly focused on the anodic corrosion process of pipeline steel. However, corrosion in soils is an electrochemical process at the metal surface. The reduction reactions of cathodic depolarizers always occur accompanied with the

dissolution process of steel. Oxygen and proton ion (H^+) have been recognized as the most common cathodic depolarizers in the corrosion process of steel in soils. Previous research has shown that corrosion in neutral/alkaline soil occurs as aerobic corrosion [15-17], and its mechanism depends essentially on the presence of oxygen. It has been generally expected that oxygen reduction is the cathodic reaction supporting the corrosion process, and the corrosion rate of steel is supposed to be proportional with the content of dissolve oxygen (DO) in the soil. In soils with higher moisture, oxygen diffusion is extremely slow and is the rate-determining step [16, 18], whereas the Ohmic overpotential caused by soil resistivity dominates the corrosion process in the low moisture soils.

However, the corrosive nature of acidic red soil is significantly different from the other soils. Red soils tend to be acidic, high water content, low oxygen content and high resistivity ($> 100 \Omega m$) because of the intensive weathering and leaching process under humid climate conditions [15, 19-20]. According to the general rule, as assessed based on oxygen content and resistivity, corrosion aggressiveness of red soils should be very mild. By contrast, as evidenced by long-term exposures in the Yingtan soil (representative of red clay soils in South China), acidic red soils are actually extremely aggressive towards ferrous metal. The corrosion rate of carbon steel in red soil is above 0.1 mm/y [21]. Hence, for the corrosion of steel in acidic red soil, other important factors may exist but have not been taken into account. Many studies showed that oxygen reduction is not a dominant cathodic reaction in the corrosion processes of steel in anoxic conditions. Moreover, the pH values of red soils are in the range of 3.5-5.0 [20, 23]. According the general corrosion theory, the corrosion mechanism of steel may be changed to hydrogen depolarization combined with the consumption of oxygen. Our previous study [24] found that DO accelerated the cathodic corrosion process of X80 steel in acidic soil simulated solution with pH 4.0. However, so far, the corrosion mechanism of X80 steel in acidic soil simulated solution under various conditions, especially for the cathodic reaction, has not yet been elucidated.

Hydrogen collection is especially important in the corrosion process dominated by hydrogen depolarization. Many researchers designed a series of hydrogen collection setups [25-27]. Inverted funnel equipment is the conventional hydrogen-collecting system; that can easily lead to errors in the measurements due to the leaking of hydrogen and the variation of system temperature. Frankel [25] designed a device along with data from simultaneous polarization and hydrogen collection, but it showed larger errors for collecting small amounts of hydrogen. Wang [26] et al. obtained the average hydrogen evolution (HE) data for pure Mg in NaCl and Na_2SO_4 solution based on the generation/collection and feedback modes of scanning electrochemical microscopy (SECM). According to the above introduction, a simple and reliable hydrogen-collecting system based on the inverted funnel equipment was designed.

In this work, the hydrogen gas generated from the corrosion process of X80 steel in acidic soil simulated solution with various conditions was collected accurately by the homemade hydrogen collecting system. Based on the hydrogen evolution data, the contributions of oxygen reduction and proton ion (H^+) reduction on the corrosion of X80 steel are analyzed. Besides, polarization curve was used to determine the corrosion mechanism of X80 steel in acidic soil simulated solution.

2. EXPERIMENTAL

2.1. Materials and solution

X80 pipeline steel, with the chemical composition (wt. %) shown in Table 1, was used as the test material in this work. The X80 steel was cut into 10 mm × 10 mm square specimens, and these were embedded in epoxy resin to act as the working electrode for the electrochemical measurements. Another series of 20 mm × 20 mm × 20 mm samples were used for the immersion test. These specimens were successively abraded with SiC emery papers, rinsed with distilled water for 2 min, ultrasonicated in alcohol for 10 min, and dried in an air flow.

Yingtang (28°15' N, 116°55' E) is regarded as the representative region of acidic red clay soil in South China. The simulated solution is prepared according to the data obtained by the analysis of Yingtang soil [17, 23, 24, 28]. The solution contains 0.0468 g/L NaCl, 0.0111 g/L CaCl₂, 0.0197 g/L MgSO₄·7H₂O, 0.0142 g/L Na₂SO₄, 0.0151g/L NaHCO₃ and 0.0293g/L KNO₃. Additionally, the solution pH is adjusted to 3.0-5.0 by the addition of sulfuric acid or 1 mol/L NaOH solution. Ultra-high purity argon gas and oxygen gas (>99.99%) were charged into simulated solution to adjust the DO concentration. The oxygen content in solution was measured by a DO meter (STARTER 300D, unit. 0.01 ppm).

Table 1. Chemical composition (wt.%) of X80 steel

C	Si	Mn	P	Mo	Nb	Ti	Cr	Ni	Cu	Al	Fe
0.036	0.197	1.771	0.012	0.184	0.110	0.019	0.223	0.278	0.220	0.021	bal.

2.2. Hydrogen collection system

In this work, a simple and reliable hydrogen-collecting setup is designed on the basis of the inverted funnel equipment, as shown in Fig. 1. To verify the reliability of the homemade hydrogen collection setup, HE volume and the weight loss of X80 steel were compared by immersing in 1.3 mol/L HCl solution. Theoretically, 1 mol H₂ would be formed when 1mol Fe was consumed in the HCl solution, and the correlation coefficient K₀ should be 0.4 mL/mg. Fig. 2 shows the curves for the relationship between HE volume and the steel weight loss for X80 steel immersed in the HCl solution. As shown in Fig.2, the correlation coefficient (K₁) fitted on the basis of the actual test data was 0.378 mL/mg. K₁/K₀ was about 94.5 %, indicating that the hydrogen collection efficiency was quite good. This minor error might be caused by the fraction of hydrogen dissolved in the solution combined with the depletion of oxygen in the closed system. In general, the homemade hydrogen collection device could accurately collect minute quantities of hydrogen induced by the corrosion of X80 steel.

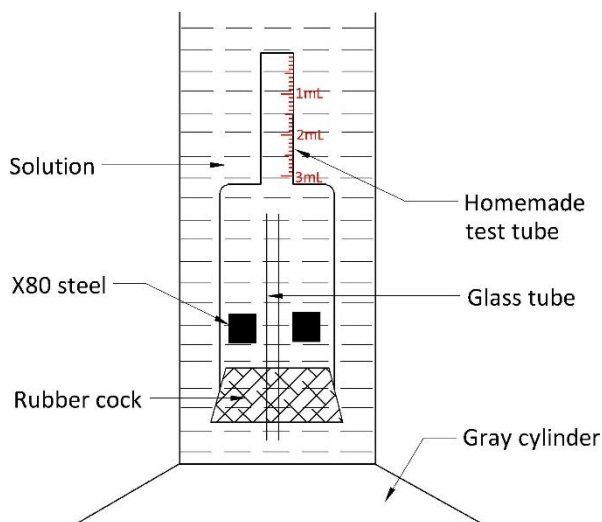


Figure 1. Schematic of hydrogen collecting setup during static corrosion

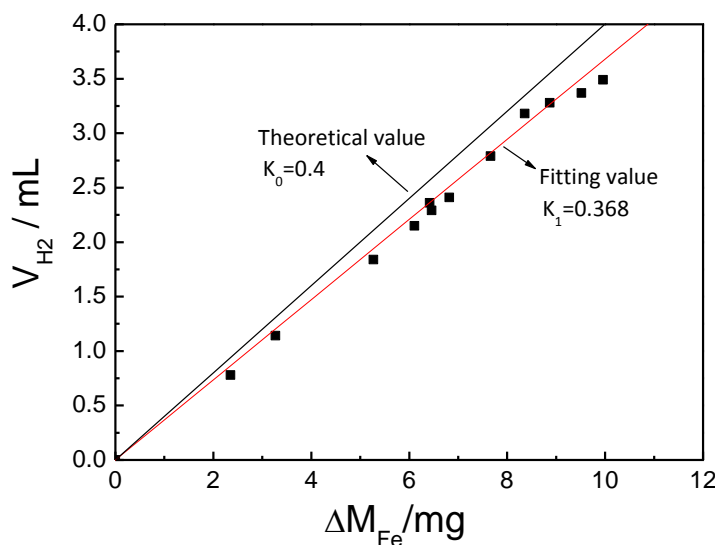


Figure 2. Relationship curve between HE volume and the weight loss of X80 steel during immersing in HCl solution.

2.3. Immersion test

X80 steel specimens are immersed in the acidic soil simulated solution at 30 °C. HE volume was measured during static corrosion using the homemade hydrogen-collecting system, defined as V_{H_2} (mL). Furthermore, the variation of DO concentration during the corrosion was measured by a DO meter, denoted as $\Delta_{[DO]}$ (ppm). The weight loss of X80 steel during the corrosion was measured by analytical balance (CPA 225D) with the accuracy of 0.01mg, denoted as ΔM_{Fe} (g). i_{Fe} , i_{H_2} and i_{O_2} can be calculated according to Eqs.1-3, respectively.

$$i_{Fe} = \frac{\Delta m_{Fe} n_{Fe} F}{M_{Fe} St} \tag{1}$$

$$i_{O_2} = \frac{\Delta_{[DO]} V_{sol} n_{O_2} F}{1000 M_{O_2} S t} \quad (2)$$

$$i_{H_2} = \frac{V_{H_2} n_{H_2} F}{22400 S t} \quad (3)$$

Where, n_{Fe} , n_{H_2} and n_{O_2} are the number of electrons involved in the reactions of oxygen reduction, hydrogen evolution and iron oxidation, respectively. M_{Fe} and M_{O_2} are the molar mass of iron and oxygen (g mol^{-1}), respectively. V_{sol} is the solution volume (L). F is the Faraday's constant (96500 C mol^{-1}). S is the surface area of the sample (m^2), and t is the corrosion time (h).

2.4. Electrochemical experiments

Polarization curves of X80 steel in the acidic soil simulated solution are conducted by using an Autolab PGSTAT 302 N. The tests are performed by using a three-electrode electrochemical cell at $25 \pm 2 \text{ }^\circ\text{C}$. A saturated calomel electrode (SCE) and a platinum sheet are used as the reference and counter electrodes, respectively. X80 steel specimens were coated with epoxy resin, and an area of 1 cm^2 was left exposed for electrochemical testing. Polarization curves are obtained potentiodynamically from -2.0 V (vs. SCE) to 1.0 V (vs. SCE) at the scan rate of 1 mV/s . All tests are repeated by three duplicate specimens to confirm reproducibility of the results. Furthermore, the morphology of the corroded X80 steel was observed by a KH-7700 three-dimensional microscope.

3. RESULTS AND DISCUSSION

3.1. Thermodynamic analysis

Corrosion of X80 steel in the acidic soil environment is an electrochemical process [15, 17, 23, 24]. The anodic process of corrosion for X80 steel is the dissolution of Fe (Eq.4), and the cathodic reaction of corrosion may involve the reduction of H^+ (Eq. 5) or oxygen (Eq. 6). The equilibrium potentials of the reactions can be determined according to Nernst equation (Eqs. 7- 9) and are given by:



$$E_{\text{Fe}^{2+}/\text{Fe}}^e = -0.684 + 0.0296 \lg a_{\text{Fe}^{2+}} \text{ (V, SCE)} \quad (7)$$

$$E_{\text{H}^+/\text{H}_2}^e = -0.244 - 0.0591 \text{ pH (V, SCE)} \quad (8)$$

$$E_{\text{O}_2/\text{H}_2\text{O}}^e = 0.985 - 0.0591 \text{ pH (V, SCE)} \quad (9)$$

Open-circuit potential (OCP) values of X80 steel in the acidic soil simulated solution under various conditions are shown in Fig.3. OCP of X80 steel decreased with decreasing DO concentration at all pH. At pH=3.0, OCP values were smaller than -0.4213 V regardless of DO concentration, indicating that X80 steel simultaneously met the thermodynamic requirements of oxygen-consuming

corrosion and HE corrosion. For pH 5.0 and DO concentration smaller than 4.45 ppm, OCP was < -0.5395 V, the reduction of both O_2 and H^+ could occur theoretically. Whereas, for DO greater than 4.45 ppm at pH=5.0, OCP > -0.5395 V, HE corrosion could not occur from thermodynamics analysis. At pH=7.0, -0.6577 V $<$ OCP $<$ 0.5713 V (E_{O_2/H_2O}^e), so only oxygen-consuming corrosion could occur. Based on the thermodynamics analysis, only when DO concentration decreased to a certain extent, HE corrosion started to occur at the same pH. Meanwhile, the change of pH also could affect the criterion of HE corrosion in the solution with the same DO content. That is, the availability of HE corrosion for X80 steel in the acidic soil simulated solution depended on the combined effects of pH and DO concentration.

3.2. Hydrogen evolution volume at various conditions

Thermodynamic analysis showed that hydrogen evolution corrosion may be present in the acidic soil system. Collection of hydrogen gas was helpful to quantitatively analyze the corrosion process of X80 steel. Fig.2 had demonstrated that the efficiency of the homemade hydrogen collection apparatus was quite good.

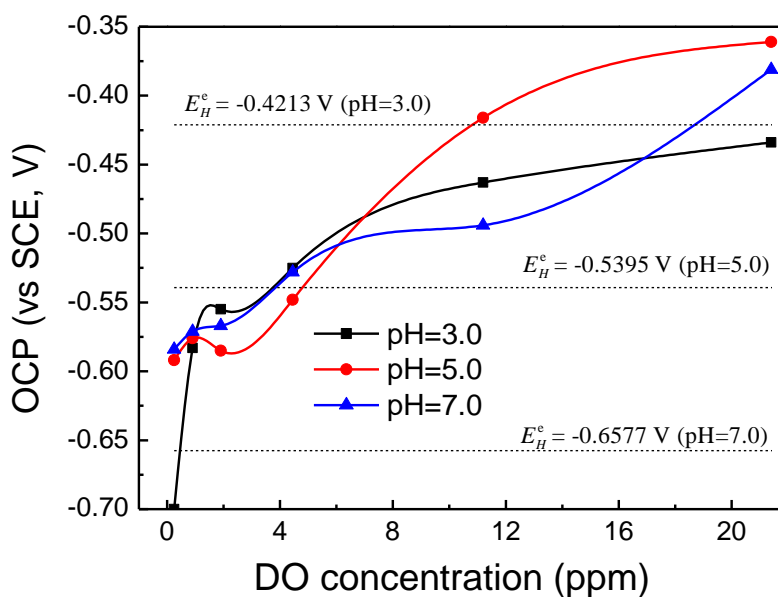


Figure 3. OCP of X80 steel in the acidic soil simulated solution under various conditions.

Fig.4 shows the volume of hydrogen gas measured at 24h for X80 steel immersed in the simulated solution under various conditions. It could be seen that the hydrogen evolution volume obviously varied with DO concentration, regardless of pH. At pH=3.0, the volume of hydrogen gas was larger and gradually increased with the decrease of DO concentration, indicating that oxygen-consuming corrosion and hydrogen evolution corrosion occurred simultaneously. When DO was adequate, oxygen-consuming corrosion occurred preferentially, and so the HE volume was relatively low. For pH 4.0 and DO concentration larger than 2.00 ppm, HE volume did not change substantially

with DO concentration, indicating that oxygen-consuming corrosion was the main cathodic reaction in this status. However, HE volume increased sharply when DO was reduced to 1.50 ~0.40 ppm, showing that HE corrosion occurred and gradually dominated the cathodic process. In the system with pH 5.0, only a small amount of hydrogen gas was collected when DO was less than 1.50 ppm, indicating that HE corrosion may be present. By contrast, almost no hydrogen gas was collected for the solution with a high DO concentration, and the proportion of HE corrosion was very low.

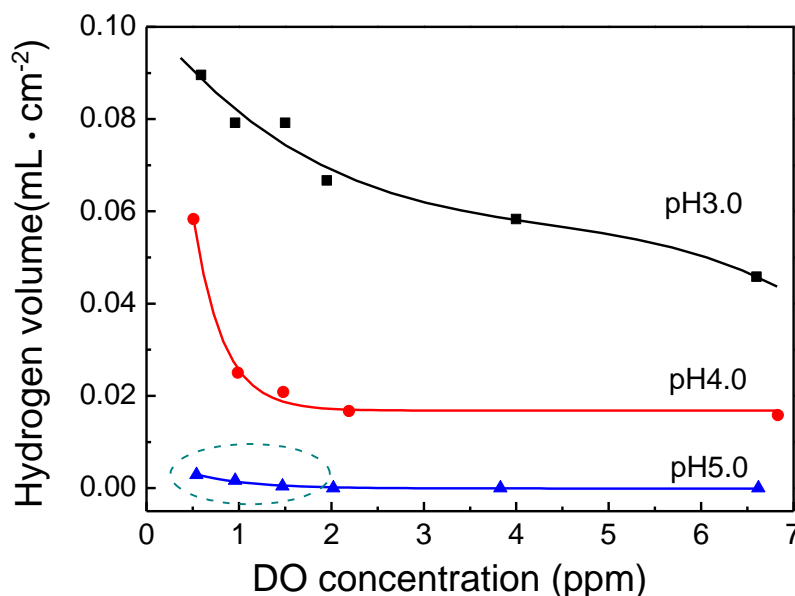


Figure 4. The volume of hydrogen gas measured at 24h for X80 steel immersed in the simulated solution under various conditions.

3.3. Kinetics of oxygen reduction and hydrogen evolution

Fig.5 shows the HE volume and oxygen-consuming volume when X80 steel was immersed in the simulated solution with different pH and 6.90 ppm DO. The current density of iron oxidation, oxygen reduction and hydrogen evolution at different times were calculated according to Eqs.1-3, as shown in Fig.6. Fig.7 gives the curves of i_{O_2}/i_{Fe} at different pH. As shown in Fig.5 and Fig.7, HE volume and oxygen-consuming volume gradually increased, and i_{O_2}/i_{Fe} gradually decreased with the longer immersion time at all pH. The variation of i_{O_2}/i_{Fe} and HE volume sufficiently indicated that oxygen-consuming corrosion occurred preferentially when X80 was immersed in the acidic soil simulated solution, and the proportion of hydrogen depolarization reaction and HE volume increased with the DO consumption.

As shown in Fig.6, the intersection of i_{H_2} and i_{O_2} moved toward higher pH with the increase of corrosion time. According to mixed-potential theory, HE rate is equal to the oxygen reduction rate at the point of intersection of i_{H_2} and i_{O_2} [29]. Therefore, the extension of immersion time, that is the decrease of DO concentration in the corrosion process, caused HE potential to move positively and HE

overpotential to decrease. Additionally, the oxygen reduction rate did not substantially change with pH at the same corrosion time, whereas HE rate greatly increased with the decrease of pH. That is, the proportion of HE corrosion increased as the pH decreased.

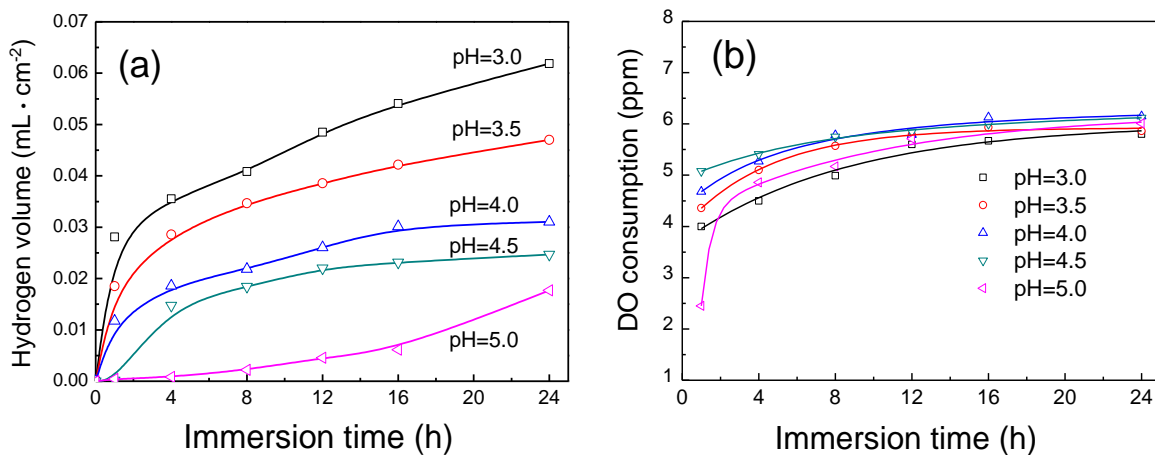


Figure 5. HE volume (a), oxygen consumption (b) for X80 steel immersing in the simulated solution with different pH and 6.90 ppm DO.

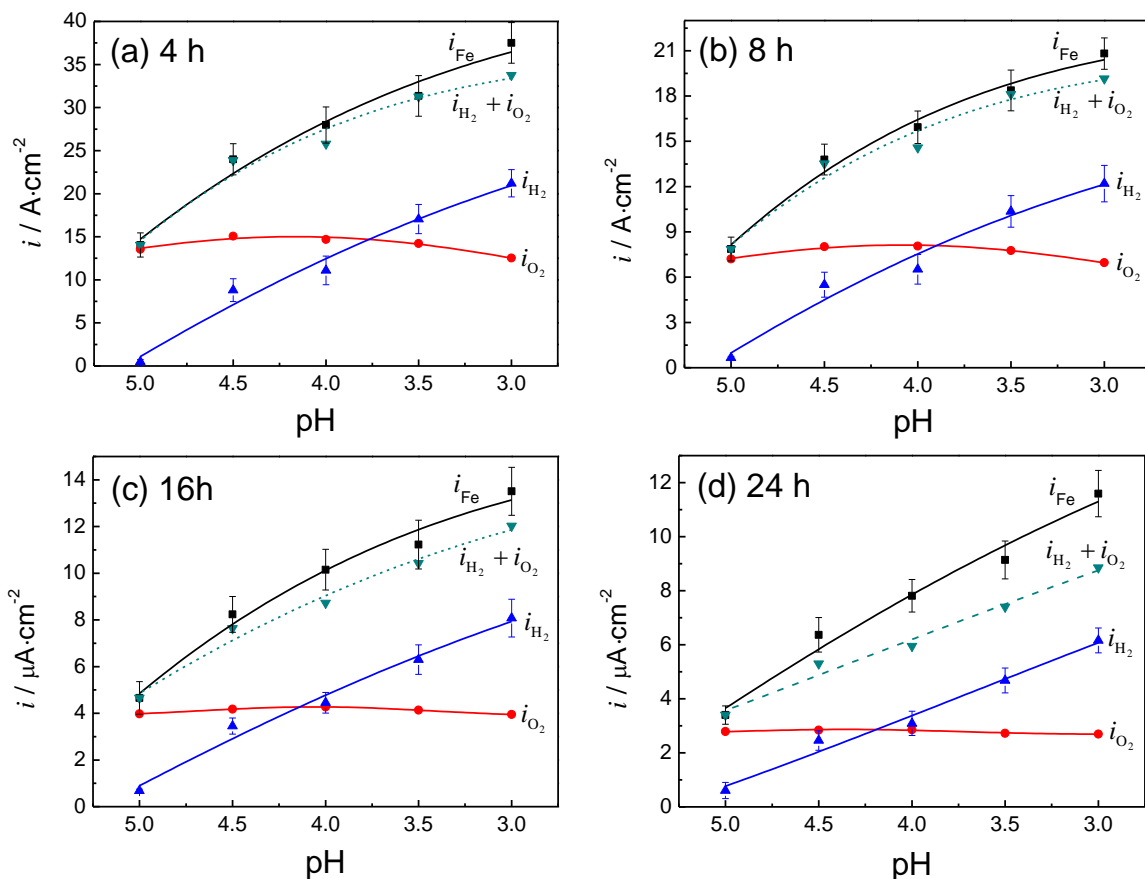


Figure 6. The current density of iron oxidation, oxygen reduction and hydrogen evolution for X80 steel immersing in simulated solution at different time.

In addition, i_{O_2} / i_{Fe} was smaller and HE volume was larger for lower pH at the same immersion time. In the solution of pH 5.0, i_{O_2} / i_{Fe} was upto 85%~95%, indicating that the oxygen reduction reaction was the main cathodic process[30-32]. When pH was 3.5 and 3.0, the volume of hydrogen gas was larger, and i_{O_2} / i_{Fe} was always less than 50%, showing that the hydrogen reduction reaction may dominate the cathodic process. However, at pH=4.0, i_{O_2} / i_{Fe} was above 50% at the initial stage (0-8h), and i_{O_2} / i_{Fe} was decreased gradually to less than 50% with increasing immersion time. The reasonable explanation was that oxygen-consuming corrosion mainly occurred at the oxygen-adequate system, and HE corrosion dominated as the corrosion progressed.

In the short-term (4-16h), $i_{H_2} + i_{O_2} \approx i_{Fe}$, the total rate of HE and oxygen reduction was balanced by the Fe dissolution rate. The hydrogen collection efficiency was quite good. However, oxygen in a closed corrosion system could be completely depleted after 24h, and the DO concentration was only 0.90 ppm. Herein, the volume of collected hydrogen was slightly smaller because a fraction of hydrogen gas dissolved in the solution, and $i_{H_2} + i_{O_2}$ was less than i_{Fe} at 24h.

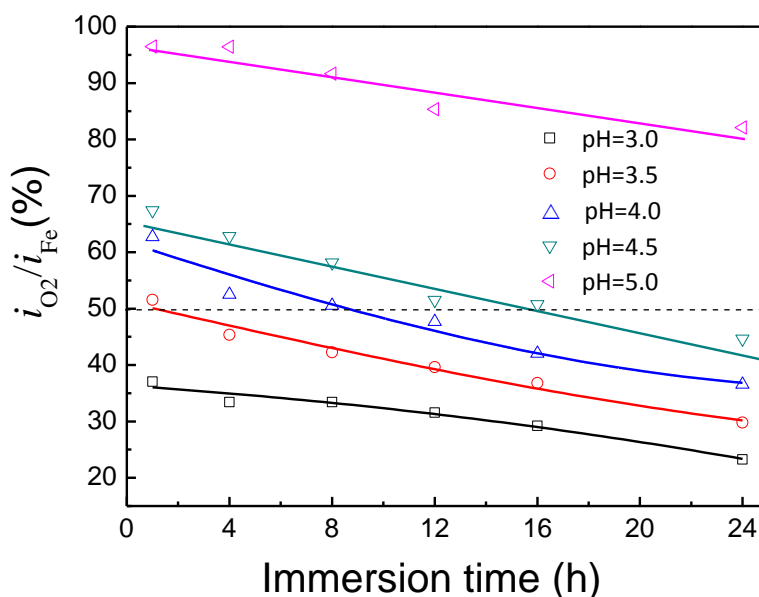


Figure 7. i_{O_2} / i_{Fe} for X80 steel immersing in the simulated solution with different pH.

3.4. Polarization curves of X80 steel under various conditions

Immersion testing in a closed system showed that the corrosion cathodic process of X80 steel in the acidic soil simulated solution was closely related to pH, DO concentration and corrosion time. To further illustrate the impact of DO concentration and pH on the corrosion behavior of X80 steel, the polarization curves of X80 steel in the acidic soil simulated solution with various conditions are shown in Fig. 8. According to the mixed-potential theory, the polarization curves can be viewed as the linear superposition of the oxidation reaction of Fe and the reduction reactions of O_2 and H^+ [29, 33, 34]. If

cathodic reaction was accelerated, the corrosion potential (E_{corr}) of X80 steel would rise, and the corrosion current density (i_{corr}) would increase.

In the system with pH 5.0, E_{corr} showed a downward trend, and i_{corr} reduced with the decrease of DO, indicating that the presence of oxygen accelerated the corrosion of X80 steel. Here, the depolarization reaction of oxygen was the main cathodic process. At the oxygen-adequate system (DO > 2.0 ppm), the relationship between the cathode overpotential and the current density met a linear law, the corrosion rate depended on the discharge process of oxygen on electrode surface. Additionally, a stable and compact corrosion product layer could be easily formed in the oxygen-consuming corrosion system [24, 35], which inhibited the anodic process of corrosion [36]. Therefore, obvious passivity characteristics were present on the anodic branch of polarization curves in the oxygen-sufficient conditions. However, the oxygen diffusion process dominated the cathodic process in the anoxic condition (DO = 0.90~0.25 ppm), as demonstrated by the presence of cathodic limiting diffusive current [37]. The corrosion rate of X80 steel was equal to the limit diffusion current of oxygen ($i_c = i_L = nFD_{O_2} \frac{[O_2]}{\delta}$) [29, 37].

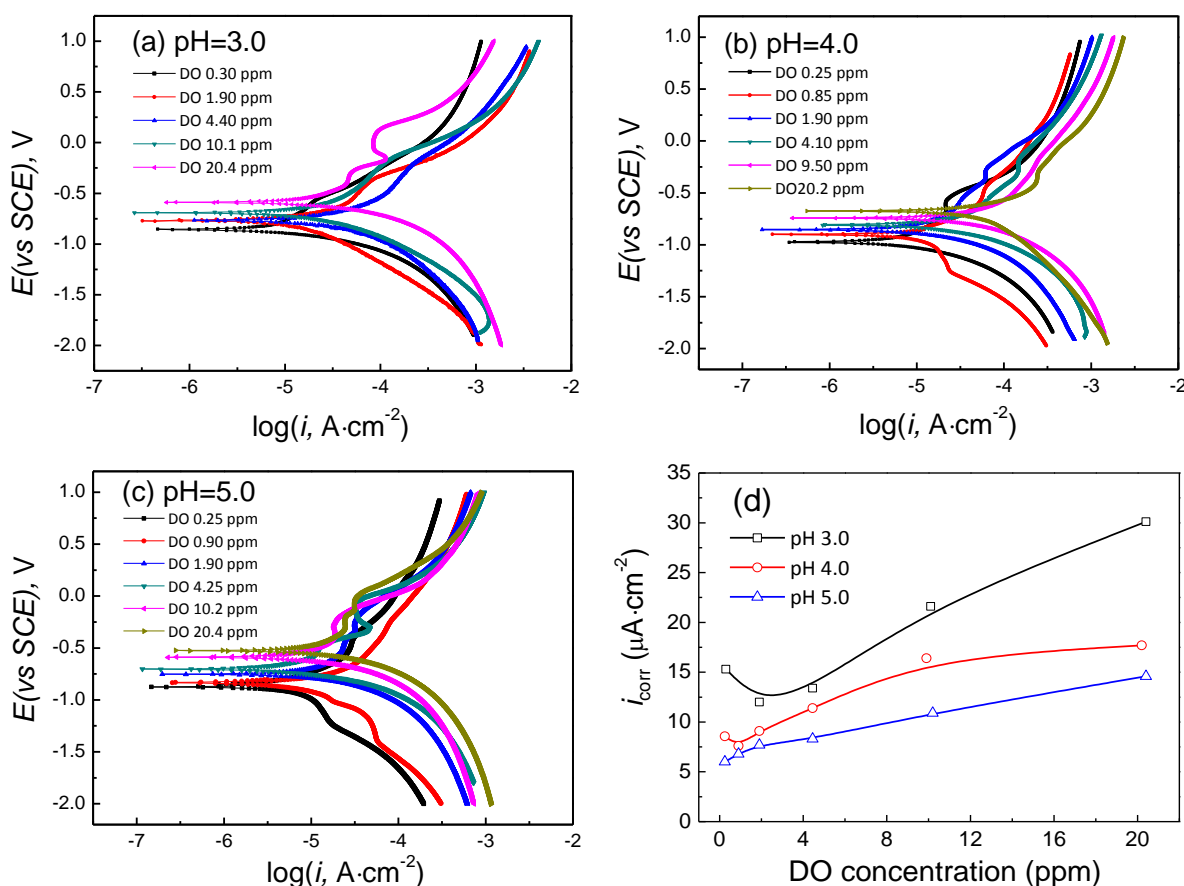


Figure 8. Polarization curves of X80 steel in acidic soil simulated solution under various conditions (a) pH 3.0, (b) pH 4.0, (c) pH 5.0 and the fitting results of corrosion current density (d).

For pH 4.0, the cathodic reaction of corrosion was closely related to DO concentration. At the high DO concentration (20.4~2.0 ppm), the cathodic branch of polarization curves was in accordance with linear polarization, E_{corr} and i_{corr} decreased with decreasing DO concentration, which comprehensively showed that oxygen-consuming corrosion mainly occurred. When DO was reduced to 0.85 ppm, a weak limiting diffusion platform appeared on the cathodic polarization curves, indicating that the corrosion process was affected by the oxygen diffusion[37]. However, the cathodic curve was again in activation control for a DO concentration of 0.25ppm, and i_{corr} slightly increased. The reasonable explanation for this phenomenon was that HE corrosion dominated the cathodic process in the deaeration environment.

The corrosion of X80 steel exhibited electrochemical activation control at pH=3.0, regardless of DO concentration. Besides, E_{corr} continuously decreased, indicating that the depolarization reaction of oxygen was inhibited as DO decreased. Whereas, the proportion of hydrogen reduction was much larger than that of oxygen reduction when DO concentration was smaller than 1.90 ppm. Here, the cathodic process was accelerated due to the occurrence of HE. Therefore, i_{corr} first decreased sharply and then increased slowly with the decrease of DO.

3.5. Analysis of corrosion mechanism

Polarization curve analysis results were consistent with the immersion data. The results fully demonstrated that oxygen-consuming corrosion occurred preferentially, and the HE corrosion subsequently appeared together with the oxygen consumption. The cathodic corrosion reaction for X80 steel in acidic soil solution was not only related to the oxygen reduction reaction, but also involved the reduction of hydrogen ions.

When pH was 3.5~3.0, the corrosion of X80 steel was accompanied by copious hydrogen evolution, and $i_{\text{O}_2} / i_{\text{Fe}}$ was always less than 50%, regardless of DO concentration (Fig.7). Here, oxygen-consuming corrosion and HE corrosion occurred simultaneously, but the proportion of hydrogen evolution corrosion was above 50% and increased with decreasing DO concentration.

In the system of pH 5.0, $i_{\text{O}_2} / i_{\text{Fe}}$ was about 85%~95%, and oxygen reduction was the cathodic reaction supporting the corrosion process. At the oxygen-adequate system, the relationship between the cathode overpotential and the current density followed a linear law, the corrosion rate depended on the oxygen ionization process. In the anoxic conditions (DO = 0.90~0.25 ppm), the oxygen diffusion process dominated the cathodic process, as demonstrated by the presence of cathodic limiting diffusive current (see Fig. 8c).

At pH=4.0, the cathodic reaction of corrosion mightily depended on DO concentration. DO concentration was higher than 1.90 ppm, $i_{\text{O}_2} / i_{\text{Fe}} > 50\%$, the cathodic branch of polarization curves were in accordance with linear polarization, indicating that the depolarization of oxygen was still the main cathodic reaction. DO concentration was 0.85 ppm, a weak limiting diffusion platform appeared on the cathodic polarization curves, therefore the corrosion process was affected by the oxygen diffusion. When DO concentration decreased to 0.25 ppm, hydrogen reduction reaction dominates the cathodic process, and i_{corr} increased slightly.

4. CONCLUSION

1) The availability of hydrogen evolution (HE) corrosion for X80 steel in acidic soil simulated solution depended on the combined effects of pH and DO concentration. Oxygen-consuming corrosion occurs preferentially in the aerobic solution. The contribution of hydrogen reduction reaction increased with the consumption of DO.

2) In the system of pH 5.0, i_{O_2}/i_{Fe} was about 85%~95%, and oxygen reduction was the cathodic reaction supporting the corrosion process. At the oxygen-adequate system, the corrosion rate of X80 steel depended on the discharge process of oxygen on the electrode surface; whereas, oxygen diffusion process was the rate-determining step in the anoxic conditions (DO = 0.90~0.25 ppm).

3) For pH 4.0, the cathodic reaction was strongly dependent on DO concentration. DO concentration was higher than 1.90 ppm, $i_{O_2}/i_{Fe} > 50\%$, the depolarization of oxygen was still the main cathodic reaction. However, hydrogen reduction reaction dominated the cathodic process when DO was 0.25 ppm.

4) At pH=3.0, the corrosion of X80 steel was accompanied by copious HE, and i_{O_2}/i_{Fe} was always less than 50% regardless of DO concentration. Here, both the reduction reactions of O_2 and H^+ were present, but the contribution of hydrogen reduction was the key factor.

ACKNOWLEDGEMENTS

The authors are grateful to the National Natural Science Foundation of China (No. 51161021) for support to this work.

References

1. I.S. Cole, D. Marney, *Corros. Sci.*, 56 (2012) 5–16.
2. X. G. Li, D. W. Zhang, Z.Y. Liu, Z. Li, C. W. Du, C. F. Dong, *Nature*, 527(2015) 441-442.
3. J.L. Alamilla, M. A. Espinosa-Medina, E. Sosa, *Corros. Sci.*, 51 (2009) 2628-2638.
4. Z. Liu, X. Li, Y. Zhang, C. Du, *Acta Metall. Sin. (Engl. Lett.)*, 22 (2009) 58-64.
5. M. C. Yan, J. Q. Wang, E. H. Han, W. Ke, *Corros. Sci.*, 50 (2008) 1331-1339.
6. T.J. Moore, C.T. Hallmark, *Soil Sci. Soc. Am. J.*, 51 (1987) 1250-1256.
7. A. Osella, A. Favetto, *J. Appl. Geophys.*, 44(2000) 303-312.
8. A. M. El-Shamy, M. F. Shehata, A. I. M. Ismail, *Appl. Clay Sci.*, 114(2015) 461-466.
9. D. Nguyen Dang, L. Lanarde, M. Jeannin, R. Sabot, Ph. Refait, *Electrochim. Acta*, 176 (2015) 1410-1419.
10. Y.H. Wu, T.M. Liu, C. Sun, J. Xu, C.K. Yu, *Corros. Eng. Sci. Technol.*, 45(2010) 136-141.
11. A. Benmoussa, M. Hadjel, M. Traisnel, *Mater. Corros.*, 57 (2006) 771-777
12. T. M. Liu, Y.H. Wu, S.X. Luo, C. Sun, *Mater. Corros.*, 41 (2010) 228–233.
13. L. Zhang, X. G. Li, C. W. Du, *J. IronSteel Res. Int.*, 16 (2009) 52-57.
14. B. He, P. Han, C. Lu, X. Bai, *Eng. Fail. Anal.*, 58 (2015) 19-30.
15. M. C. Yan, C. Sun, J. Xu, J. H. Dong, W. Ke, *Corros. Sci.*, 80 (2014) 309- 317.
16. C.P. Gardiner, R.E. Melchers, *Corros. Sci.*, 44 (2002) 2665-2673.
17. M. C. Yan, C. Sun, J. Xu, W. Ke, *Ind. Eng. Chem. Res.*, 2014, 53, 17615-17624.
18. C.P. Gardiner, R.E. Melchers, *Corros. Sci.*, 44 (2002) 2665-2673.
19. J.-Y. Li, R.-K. Xu, H. Zhang, *J. Soil. Sediment.*, 12 (2012) 876-887.
20. R. Xu, A. Zhao, Q. Li, X. Kong, G. Ji, *Geoderma*, 115 (2003) 75-84.
21. C.N. Cao, *Material Corrosion in Natural Environment of China*, Chemical Industry Press, Beijing,

- 2005 (in Chinese).
22. M. Barbalat, D. Caron, L. Lanarde, M. Meyer, S. Fontaine, F. Castillon, J. Vittonato, P. Refait, *Corros. Sci.*, 73 (2013) 222-229.
 23. M. C. Yan, C. Sun, J. Xu, W. Ke, *Int. J. Electrochem. Sci.*, 10 (2015) 1762-1776.
 24. S. X. Wang, D. X. Liu, N. Du, Q. Zhao, S. Y. Liu, J. H. Xiao, *Int. J. Electrochem. Sci.*, 10 (2015) 4393-4404.
 25. G. S. Frankel, A. Samaniego, N. Birbilis, *Corros. Sci.*, 70(2013) 104-111.
 26. X.Y. Wang, Y. Xia, Y. R. Zhou, L. L. Nie, F. H. Cao, J. Q. Zhang, C. N. Cao, *Acta Metall. Sin.*, 51(2015) 631-640 (in chinese).
 27. D. M. Dražić, J. P. Popić, *J. Appl. Electrochem.*, 29 (1999) 43-50.
 28. X. Chen, C. W. Du, X. G. Li, C. He, P. Liang, L. Lu. *Int. J. Miner. Metall. Mater.*, 103(2007) 9-13.
 29. Cao C N. *Principles of Electrochemistry of Corrosion, Third Edition*. Beijing: Chemical Industry Press, 2008.(in Chinese).
 30. Y. Li, J. Wu, D. Zhang, Y. Wang, B. Hou, *J. Solid State Electrochem.*, 14 (2010) 1667-1673.
 31. L. Cáceres, T. Vargas, L. Herrera, *Corros. Sci.*, 51 (2009) 971-978.
 32. L. Cáceres, T. Vargas, M. Parra, *Electrochim. Acta*, 54(2009) 7435-7443.
 33. Y. Li, D. Zhang, J. Wu, *J. Ocean Univ. China (Oceanic and Coastal Sea Research)*, 9(2010) 239-243.
 34. A. Gajek, T. Zakroczymski, *J. Electroanal. Chem.*, 578 (2005)171-182.
 35. W.C. Baek, T. Kang, H. J. Sohn, Y. T. Kho. *Electrochim. Acta*, 46 (2001) 2321-2325.
 36. G.Z. Meng, C. Zhang, Y. F. Cheng, *Corros. Sci.*, 50 (2008) 3116-3122.
 37. A. Q. Fu, X. Tang, Y. F. Cheng, *Corros. Sci.*, 51(2009) 186-190.

© 2016 The Authors. Published by ESG (www.electrochemsci.org). This article is an open access article distributed under the terms and conditions of the Creative Commons Attribution license (<http://creativecommons.org/licenses/by/4.0/>).